Dnt1 acts as a mitotic inhibitor of the spindle checkpoint protein dma1 in fission yeast

Yamei Wang[a,*], Wen-zhu Li[a,*], Alyssa E. Johnson[b,*], Zhou-qing Luo[a,*], Xue-li Sun[a], Anna Feoktistova[b,c], W. Hayes McDonald[d], Ian McLeod[d], John R. Yates III[d], Kathleen L. Gould[b,c], Dannel McCollum[e], and Quan-wen Jin[a]

[a]School of Life Sciences, Xiamen University, Xiamen 361005, Fujian, China; [b]Department of Cell and Developmental Biology and [c]Howard Hughes Medical Institute, Vanderbilt University School of Medicine, Nashville, TN 37232; [d]Department of Cell Biology, Scripps Research Institute, San Diego, CA 93037; [e]Department of Microbiology and Physiological Systems and Program in Cell Dynamics, University of Massachusetts Medical School, Worcester, MA 01605

ABSTRACT **The *Schizosaccharomyces pombe* checkpoint protein Dma1 couples mitotic progression with cytokinesis and is important in delaying mitotic exit and cytokinesis when kinetochores are not properly attached to the mitotic spindle. Dma1 is a ubiquitin ligase and potential functional relative of the human tumor suppressor Chfr. Dma1 delays mitotic exit and cytokinesis by ubiquitinating a scaffold protein (Sid4) of the septation initiation network, which, in turn, antagonizes the ability of the Polo-like kinase Plo1 to promote cell division. Here we identify Dnt1 as a Dma1-binding protein. Several lines of evidence indicate that Dnt1 inhibits Dma1 function during metaphase. First, Dnt1 interacts preferentially with Dma1 during metaphase. Second, Dma1 ubiquitin ligase activity and Sid4 ubiquitination are elevated in *dnt1*Δ cells. Third, the enhanced mitotic defects in *dnt1*Δ *plo1* double mutants are partially rescued by deletion of *dma1*$^{+}$, suggesting that the defects in *dnt1*Δ *plo1* double mutants are attributable to excess Dma1 activity. Taken together, these data show that Dnt1 acts to restrain Dma1 activity in early mitosis to allow normal mitotic progression.**

Monitoring Editor
Rong Li
Stowers Institute

Received: Dec 19, 2011
Revised: Jul 3, 2012
Accepted: Jul 10, 2012

INTRODUCTION

In the fission yeast, *Schizosaccharomyces pombe*, the septation initiation network (SIN) triggers actomyosin contractile ring constriction once chromosomes have segregated to opposite sides of the cell (for reviews see McCollum and Gould, 2001; Krapp *et al.*, 2004). However, when cells are arrested in metaphase by the spindle checkpoint, SIN activity must be restrained to prevent premature mitotic exit and cytokinesis. Indeed, if the SIN is precociously activated in cells arrested in metaphase, cells exit mitosis prematurely (Fankhauser *et al.*, 1993; Guertin *et al.*, 2002b). To prevent precocious mitotic exit and cytokinesis, the checkpoint protein Dma1 inhibits SIN activity when cells are arrested by the spindle checkpoint (Murone and Simanis, 1996; Guertin *et al.*, 2002b).

Fission yeast Dma1 belongs to a small FHA-RING ubiquitin ligase family, comprising two human proteins—Chfr (checkpoint with FHA and RING) and Rnf8 (RING finger 8)—as well as two budding yeast proteins—Dma1 and Dma2 (Scolnick and Halazonetis, 2000; Fraschini *et al.*, 2004; Tuttle *et al.*, 2007; Brooks *et al.*, 2008; Loring *et al.*, 2008). These FHA-RING ligases negatively regulate the cell division cycle, apparently by coupling protein phosphorylation events to specific ubiquitination of target proteins (reviewed in Brooks *et al.*, 2008; Chin and Yeong, 2010). Recently a cytosolic and centrosomal protein Stil was identified as the first negative regulator of the mammalian Chfr. Stil reduces Chfr's stability and thus protein levels by increasing its autoubiquitination (Castiel *et al.*, 2011).

Dma1 contains both an FHA domain, which is essential for its localization at spindle pole bodies (SPBs) and the division site, and a RING finger (RF) domain, which confers E3 ubiquitin ligase activity

This article was published online ahead of print in MBoC in Press (http://www.molbiolcell.org/cgi/doi/10.1091/mbc.E11-12-1020) on July 18, 2012.

*These authors contributed equally to this work.

Address correspondence to: Quan-wen Jin (jinquanwen@xmu.edu.cn) or Dannel McCollum (dannel.mccollum@umassmed.edu).

Abbreviations used: 2D, two dimensional; EMM, Edinburgh minimal medium; FHA, fork-head–associated domain; GFP, green fluorescent protein; 3HA, three tandem repeats of the influenza virus hemagglutinin epitope; HU, hydroxyurea; LC, liquid chromatography; MBP, maltose-binding protein; λ-PPase, lambda phosphatase; RF, RING finger domain; RFP, red fluorescent protein; SD, standard deviation; SEM, standard error mean; SIN, septation initiation network; SPB, spindle pole body; TAP, tandem affinity purification; YE, yeast extract rich medium.

to the protein (Murone and Simanis, 1996; Guertin *et al.*, 2002b; Johnson and Gould, 2011). Dma1 localizes at the SPB through interaction with the SIN scaffold protein Sid4 and ubiquitinates Sid4 to prevent recruitment of the Polo-like kinase Plo1 during a mitotic checkpoint arrest (Chang and Gould, 2000; Guertin *et al.*, 2002a,b; Johnson and Gould, 2011). Antagonizing Plo1 recruitment to SPBs prevents SIN activation and mitotic exit. Dma1 does not seem to inhibit Plo1 function in early mitotic events such as spindle assembly, suggesting that Dma1 itself may be regulated to limit its ability to antagonize Plo1.

Fission yeast Dnt1 was first identified in a genetic screen for suppressors of the cytokinesis checkpoint defect in a weakened SIN mutant, *cdc14-118 myo2-E1* (Jin *et al.*, 2007). The majority of Dnt1 accumulates in the nucleolus throughout the entire cell cycle. The amino acid sequence of Dnt1 shows weak similarity to those of budding yeast nucleolar proteins Net1/Cfi1 and Tof2, but no clear homologues have been found in higher eukaryotes. However, unlike Net1/Cfi1, which regulates the mitotic exit network through the Cdc14 phosphatase, Dnt1 inhibits the SIN independently of Clp1, the fission yeast homologue of Cdc14 (Jin *et al.*, 2007). The detailed mechanism of Dnt1's negative regulation of the SIN has remained unclear.

In this study, we identified the protein Dnt1 as a negative regulator of Dma1 in early mitosis. Dnt1 binds to Dma1 specifically in mitosis, and loss of Dnt1 results in increased levels of Dma1 at SPBs, higher Dma1 enzymatic activity, elevated Sid4 ubiquitination, and interference with early mitotic events such as spindle assembly. *dnt1*Δ cells also display negative genetic interactions with *plo1* mutants, which are reversed by *dma1* deletion, further supporting Dnt1 as a negative regulator of Dma1. Overall, we present evidence that Dnt1 restricts Dma1 function in early mitosis in order to prevent Dma1 from interfering with normal mitotic progression.

RESULTS

Identification of Dnt1 as a Dma1-binding protein

To better understand Dma1 function, we used a tandem affinity purification (TAP) strategy (Rigaut *et al.*, 1999; Gould *et al.*, 2004) to identify potential Dma1-associated proteins from cycling *S. pombe* cells. Dma1 protein complexes were subjected to two dimensional (2D) liquid chromatography (LC) mass spectrometric analysis. One major Dma1-associated protein, Dnt1, was identified reproducibly (Figure 1A; see Supplemental Tables S2 and S3 for complete lists of copurifying proteins). Reciprocally, Dma1 was identified by 2D LC mass spectrometric analysis as a major component of purified Dnt1-TAP complexes (Figure 1A; see Supplemental Table S4 for complete list of copurifying proteins). To validate these results, we constructed a yeast strain in which Dma1 and Dnt1 were C-terminally tagged at their endogenous loci with green fluorescent protein (GFP) and 13Myc, respectively, and performed coimmunoprecipitation experiments. Our results established that Dma1-GFP stably bound Dnt1-13Myc (Figure 1B). Furthermore, by using the yeast two-hybrid system, we found that Dma1 and Dnt1 interacted with each other, suggesting that the two proteins might interact directly (Figure 1C).

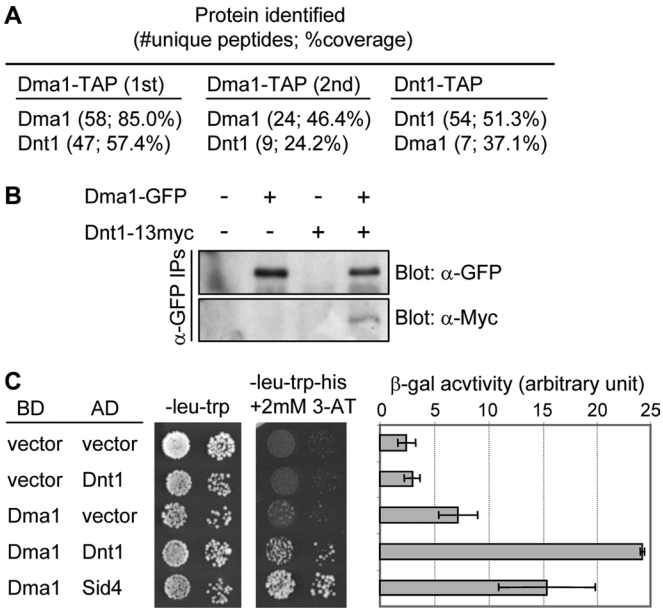

FIGURE 1: Identification of Dnt1 as a Dma1-binding protein. (A) Results of tandem mass spectrometry analysis of protein mixtures from two independent Dma1-TAP purifications (1st and 2nd) and from one Dnt1-TAP purification. (B) Confirmation of the physical association between Dma1 and Dnt1 in vivo. Lysates were prepared from unsynchronized yeast cells expressing no tags, either Dma1-GFP or Dnt1-13myc, or both Dma1-GFP and Dnt1-13myc. Dma1-GFP was immunoprecipitated, and samples were analyzed by immunoblotting using anti-GFP and anti-Myc antibodies as indicated. (C) Dma1 interacts with Dnt1 by yeast two-hybrid assay. Dma1 was fused with the DNA-binding domain of GAL4 (BD) and Dnt1 with the transcriptional activation domain of GAL4 (AD). *S. cerevisiae* host strain PJ69-4A was cotransformed with plasmids as indicated, and growth on synthetic defined medium/−Leu, −Trp and synthetic defined medium/−Leu, −Trp, −His, +2 mM 3-aminotriazole is shown (left). As controls, coexpressions of Dma1 and empty AD vector and of empty BD vector with Dnt1 (negative control) or an AD fusion with *S. pombe* Sid4 (positive control) are shown. The two-hybrid interaction between Dma1 and Sid4 has been shown previously (Guertin *et al.*, 2002b). Mean β-galactosidase activity units from liquid β-galactosidase assay are also shown (right). Error bars, SD from three independent experiments.

Dma1 and Dnt1 interaction is cell cycle dependent

Dma1 levels do not vary in abundance during the cell cycle (Guertin *et al.*, 2002b). Similarly, immunoblot analyses of cells growing asynchronously or arrested in G1, S, or metaphase indicated that Dnt1 protein levels did not change appreciably as cells progress through the cell cycle (Figure 2A). Nevertheless, we wondered whether Dma1 and Dnt1 interact at particular phases in the cell cycle. To test this, we arrested cells producing both Dma1-GFP and Dnt1-13Myc at different stages in the cell cycle using a drug (hydroxyurea [HU]) or various cell cycle mutants and subjected them to anti-GFP immunoprecipitation. Of interest, Dnt1 copurified with Dma1 the most in cells arrested in metaphase using either the proteasome mutant *mts3-1* or the β-tubulin mutant *nda3-KM311* (Figure 2A). We also explored whether the strong interaction between Dma1 and Dnt1 established at metaphase could remain into anaphase. We enriched anaphase cells by performing a block-and-release experiment using the *nda3-KM311* mutation and found that Dnt1 bound Dma1 throughout anaphase, but the interaction decreased significantly when cells underwent cytokinesis (Figure 2B). The fact that the overall levels of Dma1 and Dnt1 do not change throughout the cell cycle (Guertin *et al.*, 2002b) indicates that the ability of the two proteins to interact is cell cycle regulated.

Dma1 binds a phosphorylated form of Dnt1 in metaphase

Given that Dma1 contains a phospho-binding FHA domain, we reasoned that the interaction between the two proteins might be regulated by the phosphorylation status of Dnt1. We first tested whether

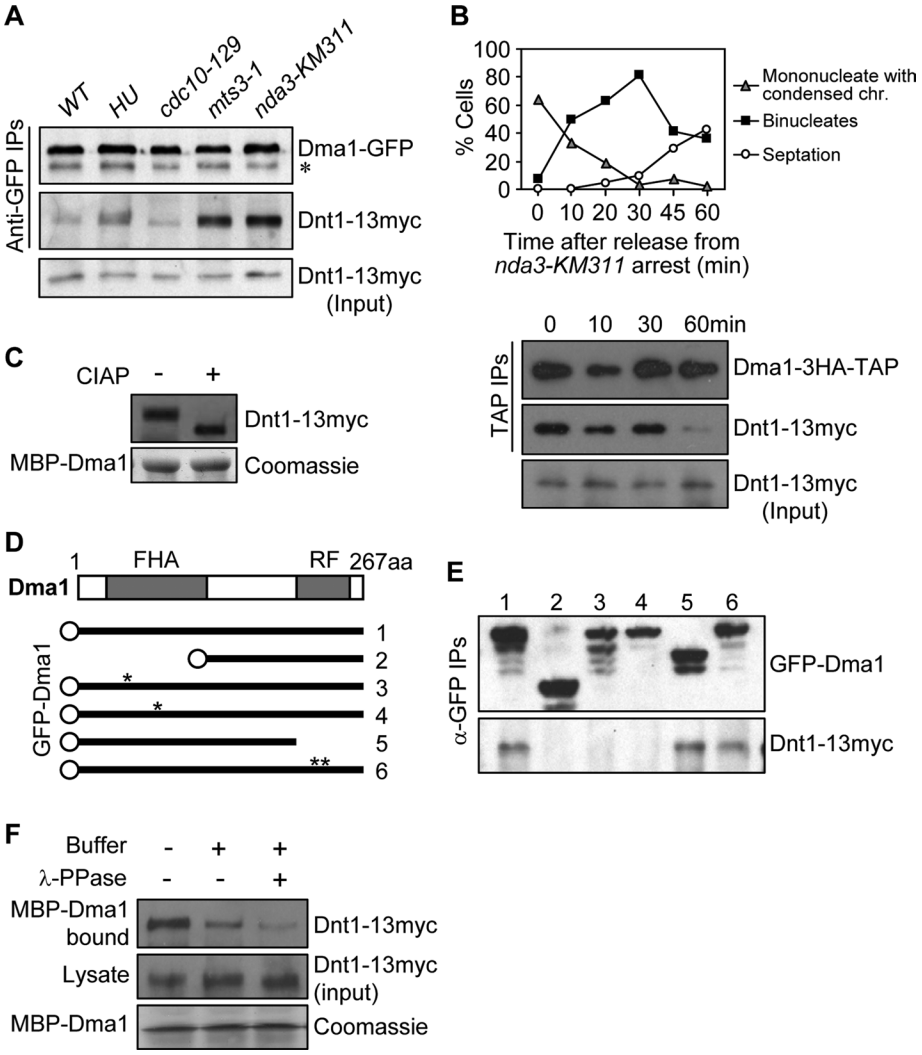

FIGURE 2: Dma1 binds phosphorylated Dnt1 in early mitosis. (A) Dma1 and Dnt1 interact strongly at the prometaphase–metaphase transition. Lysates were prepared from asynchronous *dma1-GFP dnt1-13myc* cells or cells arrested at different stages of the cell cycle (S phase by HU, G1 phase by *cdc10-129*, metaphase by *nda3-KM311* and *mts3-1*), and Dma1-GFP was immunoprecipitated and samples analyzed by Western blotting using anti-GFP and anti-Myc antibodies as indicated. The *mts3-1* and *nda3-KM311* mutations were used to arrest cells at prometaphase–metaphase transition. About 3–4% of total lysates were loaded as input to detect endogenous Dnt1-13myc. (B) Interaction between Dma1 and Dnt1 persists in anaphase. *nda3-km311 dma1-3HA-TAP dnt1-13myc* cells were first arrested at prometaphase–metaphase transition at 18°C for 6 h and released at 30°C, and samples were collected at the indicated time points. Top, cells with condensed chromosomes (indicating prometaphase–metaphase arrest), binucleate cells (indicating anaphase), or septated cells are quantified over a time course. Bottom, Dma1-3HA-TAP was immunoprecipitated, and samples were analyzed by immunoblotting using anti-hemagglutinin and anti-Myc antibodies as indicated. (C) Dma1-bound Dnt1 can be dephosphorylated in vitro. MBP-Dma1 was produced in bacteria and mixed with protein extracts prepared from *mts3-1 dnt1*-13myc cells, and the MBP-Dma1 pull-down complexes were treated with or without calf-intestinal alkaline phosphatase and analyzed by immunoblotting with anti-myc antibodies. (D, E) Dma1 and Dnt1 interact via the Dma1 FHA domain in vivo. Schematic diagrams of Dma1 variants fused to GFP are shown in D. Asterisks in D indicate the positions of point mutations (R64A [#3], H88A [#4], and C210;H212A [#6]). In E, *mts3-1 dnt1-13myc dma1*Δ cells (YDM3274) expressing the different Dma1 versions shown in D from plasmids (pREP42-*GFP-dma1*$^+$) were arrested in metaphase using *mts3-1* temperature shift, and then Dma1-GFP was immunoprecipitated, and samples were analyzed by immunoblotting using anti-GFP and anti-Myc antibodies as indicated. (F) Pretreatment of lysates prepared from *mts3-1 dnt1-13myc* yeast cells with λ-PPase caused reduced binding of Dnt1-13myc to bacteria-produced MBP-Dma1. Lysates prepared from *dnt1-13myc* yeast cells were first treated without or with λ-PPase for 75min before being mixed with bacteria-expressed MBP-Dma1 and subsequent precipitation by amylose resin.

Dma1 binds to a phosphorylated form of Dnt1. Bacterially expressed Dma1 was used to pull down Dnt1 from metaphase-arrested yeast cell lysates, and the complexes were treated with phosphatase to determine whether the fraction of Dnt1 that was pulled down by Dma1 was phosphorylated. Indeed, phosphatase treatment significantly enhanced the gel mobility of Dnt1 protein compared with the untreated sample, indicating that Dma1 can pull down a phosphorylated form of Dnt1 (Figure 2C). Next we examined whether the Dma1 FHA domain was required for the Dnt1–Dma1 interaction. Immunoprecipitation experiments using various mutant Dma1 proteins expressed in yeast cells showed that either the complete absence of the FHA domain or mutation of critical residues in the FHA domain abolished binding between Dma1 and Dnt1. In contrast, the RF domain was dispensable for their interaction (Figure 2, D and E). We also found that pretreating yeast cell lysates with phosphatase before the pull down reduced binding of Dnt1-13myc to bacterially expressed MBP-Dma1 (Figure 2F). Taken together, these results show that Dnt1 phosphorylation is important for its ability to bind to Dma1's FHA domain.

Dnt1 antagonizes Dma1 function by inhibiting its SPB localization and E3 ligase activity

As the first step to delineate the significance of the interaction between Dma1 and Dnt1, we analyzed whether Dma1 and Dnt1 affect each other's protein level or intracellular localization. Our biochemical analyses demonstrated that the abundance of both Dma1 and Dnt1 proteins was not influenced by the presence or absence of the other (Figure 3A and unpublished data), and we did not observe any changes in Dnt1-GFP localization in the nucleolus or on anaphase spindles when Dma1 was absent or overexpressed (Supplemental Figure S1). However, we noticed that Dma1-GFP seemed brighter at SPBs in *dnt1*Δ cells compared with wild-type cells. To explore more precisely whether Dnt1 affects Dma1 localization at the SPB, we quantitated Dma1-GFP fluorescence intensities relative to Sid4-RFP intensities at SPBs during metaphase when Dma1 first appeared at SPBs in *dnt1*Δ cells. Compared to *dnt1*$^+$ cells, Dma1-GFP intensities were significantly higher in *dnt1*Δ cells (Figure 3B). This result suggests that Dnt1 inhibits Dma1 localization to SPBs during metaphase. Furthermore, we examined Dma1-GFP fluorescence intensities in a G2-arrested (*cdc25-22*) population and found that there was no significant difference in Dma1-GFP

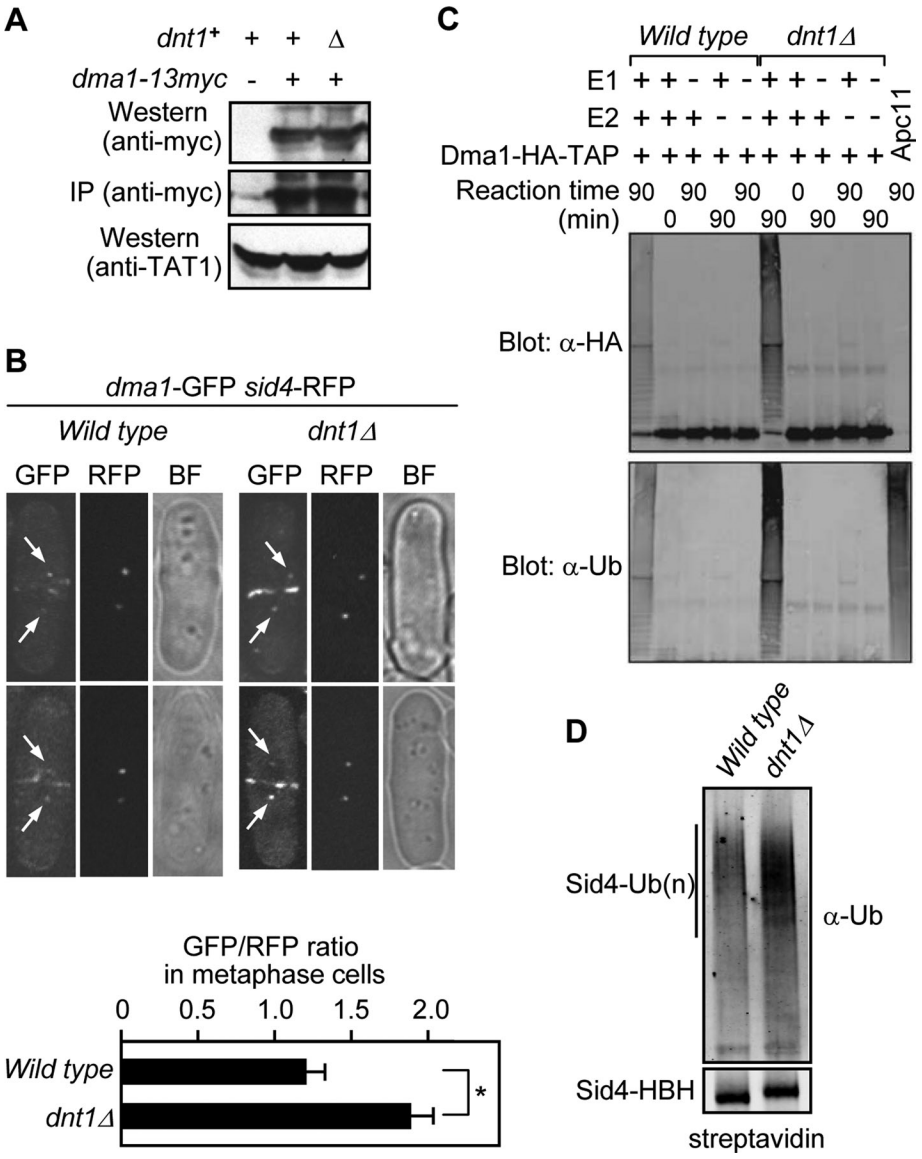

FIGURE 3: Dnt1 affects Dma1 localization at SPB and its E3 ligase activity but not its protein level. (A) Dma1 protein level is not influenced by the presence or absence of Dnt1. Wild-type or *dnt1*Δ cells with or without Dma1-13myc were cultured in liquid YE media and were collected and subjected to immunoprecipitation (with anti-myc antibodies) or straight Western assay (with anti-myc antibodies). Blot with anti-TAT1 (α-tubulin) served as a loading control. (B) Dma1-GFP intensity at SPBs is increased in *dnt1*Δ cells. Dma1-GFP and Sid4-RFP intensities were quantitated in wild-type and *dnt1*Δ cells, and final values are expressed as GFP/RFP ratio. Arrows indicate SPBs. For each cell quantitated, both SPBs were measured and averaged, for a total of 20 SPBs in 10 cells. Averaged measurements for each cell were then averaged for statistical analysis. Error bars represent the SEM; *$p < 0.05$. (C) Dma1 autoubiquitination is enhanced in *dnt1*Δ cells. Dma1-TAP was purified from metaphase-arrested (by *mts3-1* mutation) wild-type or *dnt1*Δ cells. Ubiquitin ligase assays were carried out by mixing various combinations of E1 and E2 enzymes or Dma1-TAP as shown. The reactions were allowed to proceed for 0 or 90 min at room temperature (~23°C). The Apc11 E3 enzyme is used as a control. Both Dma1 and Apc11 can autoubiquitinate. (D) Sid4 ubiquitination is increased in *dnt1*Δ cells. Sid4-HBH was purified from asynchronous wild-type or *dnt1*Δ cells under denatured conditions, and its ubiquitination status was assessed by immunoblotting with an ubiquitin antiserum and streptavidin.

intensities at SPBs in *dnt1*Δ cells compared with wild-type cells (Supplemental Figure S2A). These data suggest that the effect of Dnt1 on Dma1 localization is specific to metaphase. We also investigated Dma1 localization at SPBs when Dnt1 was overexpressed from the strong *nmt1* promoter. Although overproducing Dnt1 does not cause any obvious phenotypes in chromosome segregation and cytokinesis (unpublished data), it significantly reduced Dma1 localization at SPBs in anaphase and telophase cells (Supplemental Figure S2B).

We previously observed that Dma1 can autoubiquitinate (Johnson and Gould, 2011). If Dnt1 inhibits Dma1 ubiquitin ligase activity during early mitosis, we would anticipate that Dma1's autoubiquitination activity would be enhanced in the absence of Dnt1. To test this, we assayed the ubiquitin ligase activity of Dma1 after its purification from cells arrested in early mitosis using the proteasome mutant *mts3-1*. Consistent with Dnt1 acting as a Dma1 inhibitor, Dma1 had elevated ubiquitin ligase activity in metaphase-arrested *dnt1*Δ cells compared with metaphase-arrested wild-type cells (Figure 3C and unpublished data).

To further examine the effect of Dnt1 on Dma1 activity in vivo, we examined ubiquitination levels of the Dma1 target, Sid4. In accord with elevated Dma1 activity and SPB localization, Sid4 ubiquitination was also elevated in *dnt1*Δ cells compared with *dnt1*$^+$ cells (Figure 3D). Collectively these data suggest that Dnt1 inhibits Dma1 function by antagonizing its localization to SPBs and inhibiting its E3 ligase activity.

Absence of *dnt1*$^+$ compromises Plo1 function, which is rescued by deletion of *dma1*$^+$

Our previous study demonstrated that ubiquitination of Sid4 by Dma1 in early mitosis inhibits the polo kinase Plo1 by interfering with its localization to the SPB (Johnson and Gould, 2011). Thus we examined whether *dnt1*Δ displays negative genetic interactions with mutations in the *plo1* kinase (*plo1-24C, plo1-25, plo1-ts4*), which have been shown to be defective in spindle formation and cytokinesis (Bahler *et al.*, 1998a; Tanaka *et al.*, 2001). Double mutants between *dnt1*Δ and each *plo1* mutant had more severe growth defects compared with the single mutants, which could be partially rescued by deletion of *dma1*$^+$ (Figure 4A and Supplemental Figure S4). For *dnt1*Δ *plo1-24C*, the synthetic growth defects were also similarly rescued by removal of FHA or ring finger domains of Dma1 (Supplemental Figure S3). The *dnt1*Δ *plo1-24C* double mutants also displayed a delay in early mitosis as judged by an increase in the percentage of cells with unsegregated condensed chromosomes, which was also rescued by deletion of *dma1*$^+$ or absence of FHA or ring finger domains (Figure 4B and Supplemental Figure S3B). All these growth defects and the mitotic delay observed in *dnt1*Δ *plo1-24C* double mutants were

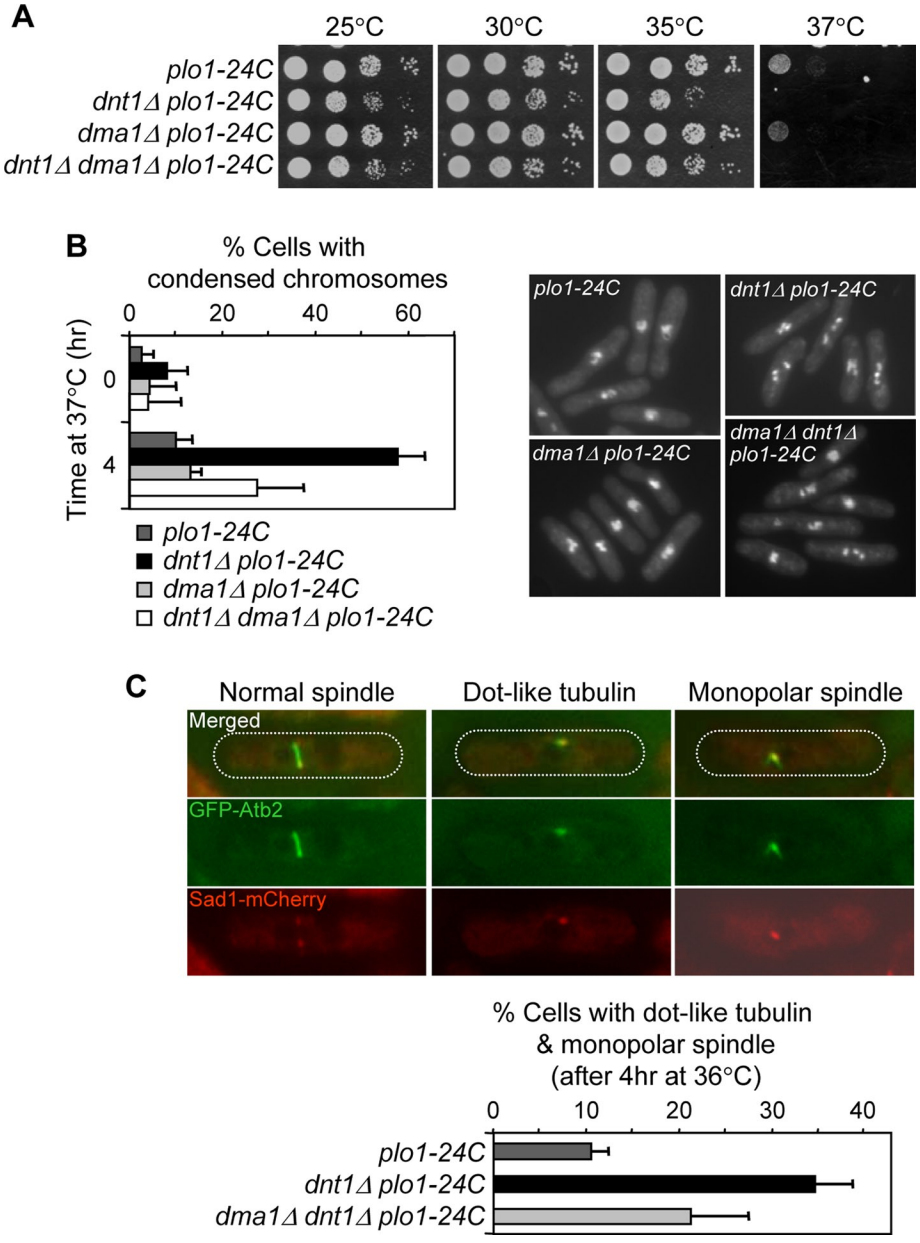

FIGURE 4: Absence of *dnt1*$^+$ compromises Plo1 function but is rescued by deletion of *dma1*$^+$. (A, B) The *plo1-24C* mutant is sensitive to deletion of *dnt1*$^+$, and the sensitivity can be alleviated by disruption of Dma1 function. (A) Serial dilutions (10-fold) of the indicated single-, double-, or triple-mutant strains were spotted on YE and incubated at the indicated temperatures. (B) Liquid cultures of the indicated strains were also grown at 25°C and then shifted to 36°C, and percentages of cells with condensed chromosomes/metaphase arrest were quantified after being fixed and stained with DAPI ($n = 200$; left). Error bars, SD from three independent experiments. Examples of mutant cells incubated at 37°C for 4 h are also shown (right). (C) Enhanced spindle formation defects in *dnt1*Δ *plo1-24C* double mutant can be partially rescued by *dma1*Δ. Liquid cultures of mutant strains carrying GFP-atb2 and Sad1-mCherry were first grown at 25°C and then shifted to 36°C for 4 h; spindle formation was visualized in live cells. Examples of mutant cells showing either normal, dot-like tubulin or a short, monopolar spindle are shown (top). Percentages of cells in each strain with defective spindles were quantified ($n = 200$; bottom). Error bars, SD from three independent experiments.

independent of Clp1 (Supplemental Figure S5), which antagonizes the positive feedback loop required for mitotic entry (Trautmann *et al.*, 2001). These results indicate that growth defects in the *dnt1*Δ *plo1* double mutants were likely caused by a metaphase arrest. Consistent with this assumption, we observed that all *dnt1*Δ *plo1-24C* cells that arrested with condensed chromosomes exhibited spindle formation defects: either a dot-like, tubulin-containing structure or a short, monopolar spindle (Figure 4C). These spindle defects were partially suppressed by deletion of *dma1*$^+$ (Figure 4C). These data show that when Plo1 function is reduced, the absence of *dnt1*$^+$ disrupts spindle formation and leads to a metaphase arrest. Taken together, these results support the notion that Dnt1 inhibits Dma1 activity in early mitosis to keep it from interfering with Plo1 function and potentially other regulators of early mitosis.

Overexpression of Dma1 in *dnt1*Δ cells causes metaphase arrest

Previous studies showed that overexpression of Dma1 caused inhibition of the SIN signaling pathway, which resulted in failed cytokinesis (Murone and Simanis, 1996; Guertin *et al.*, 2002b). Of interest, we found that deletion of *dnt1*$^+$ rendered early mitotic cells very sensitive to overexpression of Dma1, with up to 50% of cells accumulating hypercondensed chromosomes, which is typical for metaphase-arrested cells (Figure 5, A and B). This phenotype was abolished if the ring finger or FHA domain in Dma1 was deleted or key residues in these domains were mutated (Figure 5B), suggesting that the ubiquitin ligase activity of Dma1 and proper localization of Dma1 at SPB are critical for the overexpression phenotype. The presence of Cut2-GFP (securin) and Cdc13-GFP (cyclin B) signals in *dnt1*Δ cells overproducing Dma1 confirmed that these cells arrested in a preanaphase state, because these proteins are normally degraded in anaphase (Figure 5C). To test whether the mitotic arrest caused by Dma1 overexpression in *dnt1*Δ cells depends on the spindle checkpoint, we examined the effects of deleting the spindle checkpoint regulators Mad2 and Bub1. Deletion of either *mad2*$^+$ or *bub1*$^+$ suppressed the mitotic arrest caused by Dma1 overproduction (Figure 5D), demonstrating that in the absence of *dnt1*$^+$ this arrest depends on the spindle assembly checkpoint. Therefore we examined spindle organization in *dnt1*Δ cells overproducing Dma1. Consistent with our previous study (Guertin *et al.*, 2002b), overexpression of Dma1 in the presence of *dnt1*$^+$ did not impair spindle assembly (Figure 5E). However, upon Dma1 overexpression in the absence of *dnt1*$^+$, all cells that arrested with condensed chromosomes exhibited spindle formation defects. The spindle defects fell into three major classes: 1) complete failure to form a bipolar spindle, 2) a dot-like or monopolar spindle, and 3) a long spindle without segregated DNA (Figure 5F). We never observed any of these spindle formation defects in *dnt1*Δ cells without

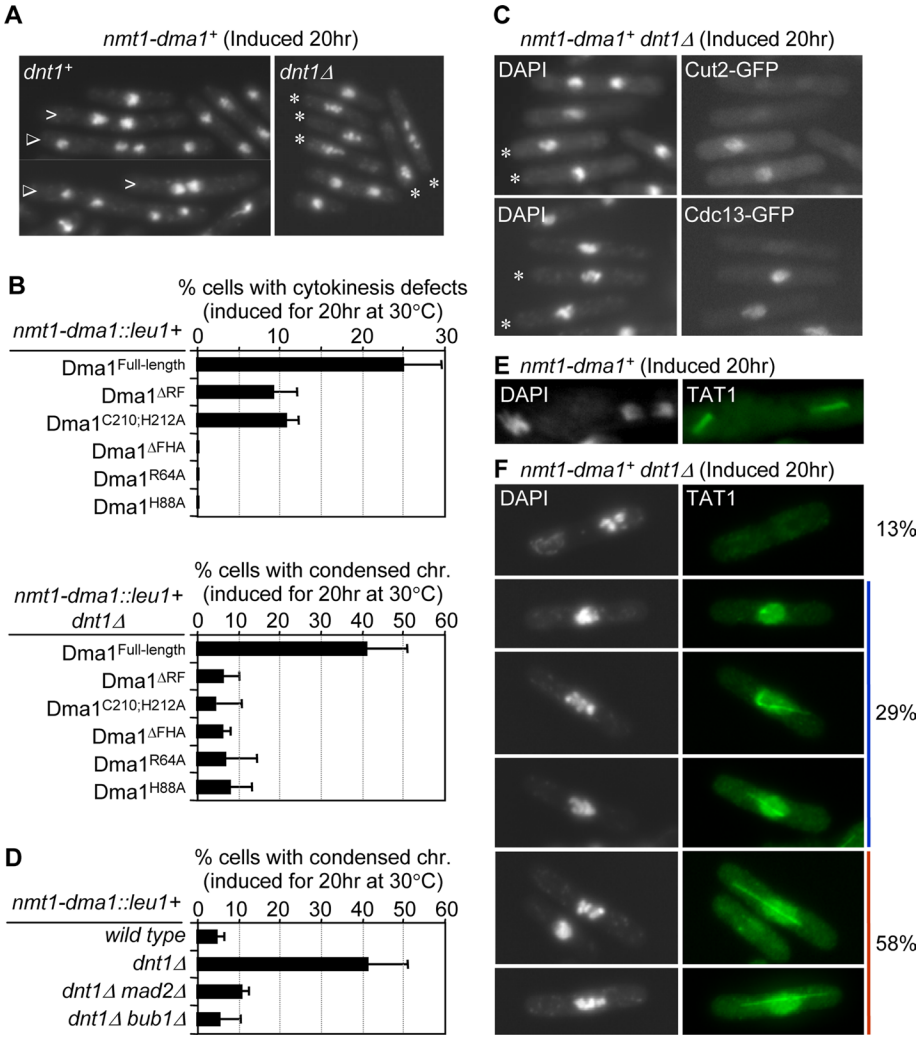

FIGURE 5: Overexpression of Dma1 in *dnt1*Δ cells leads to arrest in early mitosis. (A) Examples of *nmt1-dma1*$^+$ *dnt1*$^+$ and *nmt1-dma1*$^+$ *dnt1*Δ cells after overexpression of Dma1 in EMM liquid media without thiamine for 20 h at 30°C. Cells were fixed and stained with DAPI. In the *dnt1*$^+$ strain, open arrows and triangles indicate cells with two clustered nuclei in a postmitotic configuration and multinucleate cells, respectively. Asterisks indicate cells with condensed chromosomes in the *dnt1*Δ strain. Note that the major phenotype in Dma1-overexpressing *dnt1*$^+$ cells is defective cytokinesis, whereas cells with condensed chromosomes mainly accumulate upon overexpression of Dma1 in *dnt1*Δ. (B) The functional ring finger (RF) and FHA domains in Dma1 are required for inducing metaphase arrest when Dma1 is overproduced in *dnt1*Δ cells. The *dma1*$^+$ open reading frame with deleted RF domain (Dma1Δ^{RF}), two point mutations in RF domain (Dma1$^{C210;H212A}$), deleted FHA domain (Dma1Δ^{FHA}), or two point mutations in FHA domain (Dma1^{R64A} or Dma1^{H88A}) was integrated into the yeast genome under the full-strength *nmt1* promoter and overexpressed in wild-type or *dnt1*Δ cells. The indicated strains were fixed and DAPI stained after Dma1overexpression was induced as in A, and the frequencies of cells with cytokinetic defects (i.e., binucleate with the nuclei in a postmitotic configuration and multinucleate) and condensed chromosomes were quantified in wild-type cells or in *dnt1*Δ cells, respectively. We counted $n > 200$ cells for each strain. Error bars, SD from three independent experiments. (C) Securin Cut2 and mitotic cyclin Cdc13 persist in *dnt1*Δ cells upon overexpression of Dma1. *nmt1-dma1*$^+$ *dnt1*Δ cells carrying Cut2-GFP or Cdc13-GFP were induced for Dma1 overexpression as in A, fixed, and examined for localization of Cut2-GFP or Cdc13-GFP. Asterisks indicate cells with condensed chromosomes. (D) The phenotype of hypercondensed chromosomes in *nmt1-dma1*$^+$ *dnt1*Δ cells is dependent on the spindle assembly checkpoint. Dma1 was overexpressed in the indicated strains as in A, and cells with hypercondensed chromosomes determined by DAPI staining were counted ($n > 200$). Error bars, SD from three independent experiments. (E) Normal spindle formation upon overexpression of Dma1 in wild-type cells. Microtubules were labeled by indirect immunofluorescence with TAT1 antibody in wild-type cells induced for 20 h at 30°C for *dma1*$^+$ overexpression. Nuclei were stained with DAPI. Left, the nucleus shows condensed chromosomes at metaphase with a fully assembled spindle; right, an early-anaphase nucleus shows an intact spindle. (F) Microtubules were stained in *dnt1*Δ cells overproducing Dma1. These cells showed no spindle, partial spindles, or monopolar spindles, and the percentages of each type in cells with hypercondensed chromosomes ($n > 200$) are indicated.

overexpression of Dma1 (unpublished data). Taken together, our results suggest that the spindle formation defects and metaphase arrest phenotype in *dnt1*Δ cells overexpressing Dma1 are most likely due to a loss of Dma1 inhibition when *dnt1*$^+$ is deleted.

DISCUSSION

Dma1 mediates SIN inhibition by preventing the Polo-like kinase Plo1, an upstream activator of the SIN, from localizing to the SPB (Guertin *et al.*, 2002b). Sid4 ubiquitination by Dma1 prevents SIN activation and cytokinesis during a mitotic checkpoint arrest by delaying recruitment of Plo1 to SPBs while at the same time prolonging the residence of the SIN inhibitor Byr4 (Johnson and Gould, 2011). However, Dma1 does not seem to inhibit Plo1 function in early mitotic events such as spindle assembly, suggesting that Dma1 itself may be regulated to limit its ability to antagonize Plo1.

In this study, we identified Dnt1 as a factor that negatively regulates the extent of Dma1 recruitment to SPBs and Dma1's E3 ubiquitin ligase activity in early mitosis, possibly in response to a mitotic checkpoint. Given that we detected a strong interaction between Dma1 and Dnt1 in both metaphase and anaphase, Dnt1 might modulate Dma1 and SIN activity throughout mitosis, with the interaction in early mitosis being important for Plo1 regulation and spindle assembly. Previous studies showed that both Dma1 and Dnt1 are negative regulators of the SIN pathway (Murone and Simanis, 1996; Guertin *et al.*, 2002b; Jin *et al.*, 2007). These seemingly contradictory results could be reconciled if Dnt1 acts to inhibit Dma1 in early mitosis, and then the two proteins function together or separately to inhibit the SIN in anaphase.

Similar to mammalian polo-like kinase 1 (Plk1), Plo1 in fission yeast is critical for proper mitotic progression, and its association with the SPB is important for microtubule nucleation and function (Ohkura *et al.*, 1995; Bahler *et al.*, 1998a). Previous studies identified Sid4, Cut12, and Pcp1 as major factors that recruit Plo1 to SPBs in fission yeast (Mulvihill *et al.*, 1999; Morrell *et al.*, 2004; Fong *et al.*, 2010). On the basis of the results from the present study, we propose a model in which Dnt1 regulates Plo1 kinase through inhibition of Dma1 (Figure 6). Dnt1

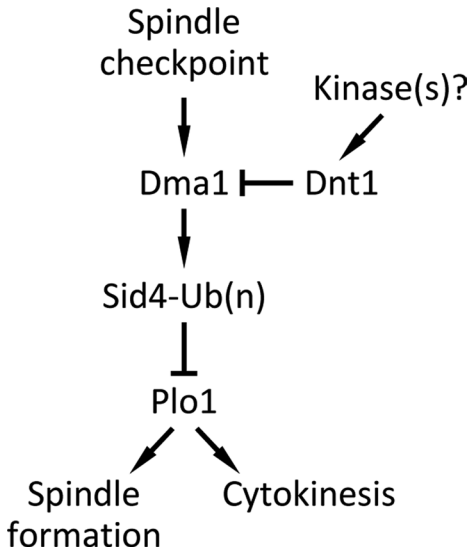

FIGURE 6: Model for Dnt1 regulation of Dma1 in early mitosis. Dnt1 is phosphorylated by an unknown kinase in prometaphase, which promotes binding of Dnt1 to Dma1 through Dma1's FHA domain. Dnt1–Dma1 interaction inhibits Dma1, which normally targets Sid4 for ubiquitination and subsequently prevents Plo1 from localization to the SPB. While at metaphase–anaphase transition, Dnt1's negative effect on Dma1 may be redirected or terminated by an unknown mechanism.

might function to fine tune Dma1 activity at the SPB to avoid problematic inhibitory effects on Plo1. However, because the rescue of the growth defects in *dnt1*Δ *plo1* double mutants by removal of Dma1 was not complete (Figure 4A and Supplemental Figure S3), there might be additional functions for Dnt1 in the regulation of the SPB and mitosis.

The mammalian protein Chfr functions in an early mitotic checkpoint that delays the cell cycle in response to microtubule-targeting drugs by inhibiting polo kinase (Plk1) and the Aurora A kinase (Scolnick and Halazonetis, 2000; Kang *et al*., 2002; Yu *et al*., 2005). Like Chfr, Dma1 also inhibits the Polo kinase Plo1 to maintain a cell cycle arrest after microtubule depolymerization (Murone and Simanis, 1996; Guertin *et al*., 2002b), although, unlike Chfr, which blocks progression into prophase (Scolnick and Halazonetis, 2000; Summers *et al*., 2005), Dma1 blocks initiation of cytokinesis. Of interest, a recent study identified a cytosolic and centrosomal protein, Stil, as the first negative regulator of the mammalian Chfr in mouse embryonic fibroblasts (Castiel *et al*., 2011). Stil limits Chfr's inhibition of Plk1 in early mitosis to allow normal mitotic progression and proper centrosome assembly by affecting Chfr's stability and protein level (Castiel *et al*., 2011). Therefore the activities of both Chfr and Dma1 seem to be carefully modulated to keep them from interfering with normal mitotic progression (Castiel *et al*., 2011, and this study). Although fission yeast Dnt1 and mammalian Stil do not show any amino acid sequence similarity, they do share similar functions in antagonizing their respective E3 ubiquitin ligase.

It is not known how Dnt1–Dma1 interaction is regulated. However, our results show that the interaction depends on Dnt1 phosphorylation. Because the interaction between the two proteins is strongest in early mitosis, when multiple kinases are active, phosphorylation of Dnt1 would provide a mechanism for the cell cycle–specific interaction between the two proteins. Clearly, finding the kinase(s) responsible for Dnt1 phosphorylation is an important goal for future studies.

In summary, we showed that in the absence of Dnt1, Dma1 can inhibit SPB function and spindle formation much like Chfr in human cells. Thus it is possible that Dma1 acts like Chfr to inhibit mitotic progression in response to certain stimuli. Because the ability of Dma1 to block mitotic progression requires loss of Dnt1, it will be interesting in future studies to determine the conditions that modulate the interaction between Dnt1 and Dma1 to regulate passage through early mitosis.

MATERIALS AND METHODS

Yeast media, strains, and genetic manipulations

The fission yeast strains used in this study are listed in Supplemental Table S1. Genetic crosses and general yeast techniques were performed as previously described (Moreno *et al*., 1991). *S. pombe* strains were grown in rich medium (yeast extract [YE]) or Edinburgh minimal medium (EMM) with appropriate supplements (Moreno *et al*., 1991). EMM with 5 μg/ml thiamine was used to repress expression from the *nmt1* promoter. YE containing 100 mg/l G418 (Sigma-Aldrich, St. Louis, MO) was used for selecting Kan^R cells. For serial dilution drop tests for growth, three serial 10-fold dilutions were made, and 5 μl of each was spotted on plates with the starting cell number of 10^4. Cells were pregrown in liquid YE or EMM at 25°C and then spotted onto YE or EMM plates at the indicated temperatures and incubated for 3–5 d before photography. *Saccharomyces cerevisiae* strain PJ69-4A was used as the host strain in two-hybrid analyses (James *et al*., 1996) and was transformed using the LiAc/PEG procedure (Gietz *et al*., 1995). Leu^+ and Trp^+ transformants were selected and scored for positive interactions by spotting onto synthetic dextrose plates lacking histidine or with 2 mM 3-aminotriazole (Sigma-Aldrich) added. Liquid β-galactosidase assays were performed as described (Pryciak and Hartwell, 1996).

Molecular biology methods

Carboxy-terminal GFP and 13Myc epitope tagging of Dnt1 was done by PCR-based gene targeting (Bahler *et al*., 1998b). To construct the *dnt1* deletion strains, the entire *dnt1*-coding region was replaced with the $ura4^+$ gene or *kanR* cassette by homologous recombination. Fission yeast cells were transformed using a lithium acetate–based procedure (Keeney and Boeke, 1994). All plasmids were generated by standard molecular biology techniques. cDNAs for two-hybrid analysis were cloned into the bait plasmid pGBT9 or the prey plasmid pGAD-XP (Clontech Laboratories, Mountain View, CA). *dma1* constructs in the pREP41-GFP expression vector were created by PCR amplification from *S. pombe* genomic DNA or subcloned from pREP42-GFP plasmids (Guertin *et al*., 2002b) using *Nde*I/*Bam*HI sites. To generate the vector for recombinant fusion protein production of MBP-dma1, a gene fragment was amplified by PCR using *S. pombe* genomic DNA, cDNA library (Clontech Laboratories), or plasmid carrying the genes as templates and then inserted into pMAL-2c (New England BioLabs, Ipswich, MA). To generate a plasmid overexpressing $dnt1^+$, we amplified the full-length 1852 nucleotide $dnt1^+$ open reading frame by PCR using *S. pombe* genomic DNA as template and then inserted it into the *Nde*I and *Xma*I sites of the pREP1 vector (Maundrell, 1993).

Strains carrying chromosomal $dma1^+$, $dma1\Delta^{RF}$, $dma1^{C210;H212A}$, $Dma1\Delta^{FHA}$, $Dma1^{R64A}$, or $Dma1^{H88A}$ expressed from the *nmt1* promoter were constructed by first cloning the *Pst*I–*Bam*HI fragments harboring the *nmt1* promoter and *dma1* from pREP1-*dma1* plasmids (Guertin *et al*., 2002b) and then subcloning them into vector pJK148 (Keeney and Boeke, 1994). The resulting plasmids were linearized and integrated at the $leu1^+$ locus by homologous

recombination as previously described for construction of *nmt1-dma1*$^{Full\text{-}length}$ (Guertin *et al.*, 2002b).

Protein methods

To prepare TAP complexes for mass spectrometry analyses, we purified Dma1-TAP and Dnt1-TAP from 8- to 10-l cultures using TAP as previously described (Gould *et al.*, 2004) and analyzed the protein composition of the complexes by 2D liquid chromatography tandem mass spectrometry as previously described (MacCoss *et al.*, 2002). For coimmunoprecipitation and Western blot experiments, whole-cell lysates were prepared in NP-40 buffer (6 mM Na_2HPO_4, 4 mM NaH_2PO_4, 1% NP-40, 150 mM NaCl, 2 mM EDTA, 50 mM NaF, 0.1 mM Na_3VO_4), and lysates were subjected to immunoprecipitation with anti-GFP (3E6; Molecular Probes, Eugene, OR) antibodies and Western blot analyses with anti-GFP or anti-Myc (9E10; Santa Cruz Biotechnology, Santa Cruz, CA) antibodies as previously described (Guertin *et al.*, 2002b). The in vivo Sid4 ubiquitination assay was performed as previously described (Johnson and Gould, 2011). Sid4 ubiquitination was detected by immunoblotting using ubiquitin antiserum (Sigma-Aldrich) and fluorescently labeled streptavidin (LI-COR Biosciences, Lincoln, NE).

In vitro binding assays

All recombinant bacterially produced MBP-Dma1 proteins were expressed in *Escherichia coli* BL21(DE3) cells and purified on amylose beads (MBP; New England BioLabs) according to the manufacturer's instructions and as previously described (Carnahan and Gould, 2003). Purified proteins were incubated with clarified whole-yeast-cell lysates made from *dnt1-13Myc* cells for 1–2 h at 4°C to examine the association between Dma1 and Dnt1. Proteins were resolved by SDS–PAGE, followed by Coomassie blue staining or Western blot analysis with anti-Myc (9E10, Santa Cruz Biotechnology) to detect proteins. Phosphatase treatment was performed either on the protein extracts pulled down by MBP-Dma1 or on yeast cell lysates before pull downs. For the phosphatase treatment after pull downs, beads were washed three times in AP buffer (50 mM Tris-HCl, pH 8.5, 1 mM EDTA) containing protease inhibitor. Either 15 U of calf-intestinal alkaline phosphatase (Fermentas, Glen Burnie, MD) or 120 U of lambda phosphatase (λ-PPase) (New England BioLabs) was added and incubated without phosphatase inhibitors (0.1 mM Na-orthovanadate, 15 mM ethylene glycol tetraacetic acid [EGTA], 5 mM NaF) for 45 min at 37°C or for 75 min at 30°C, respectively. For the phosphatase treatment before pull downs, yeast cell lysates from *dnt1-13Myc* cells were incubated with 480 U of PPase (New England BioLabs) and without phosphatase inhibitors for 75 min at 30°C, then mixed with bacterially produced MBP-dma1 for in vitro affinity binding using amylose beads as described.

In vitro ubiquitination assay

Dma1-HA-TAP complexes were purified as described (Tasto *et al.*, 2001) except that the final 1-ml elution contained 40 mM EGTA. A 5.8-µl amount of each eluate was incubated with 100 nM E1 enzyme (Boston Biochemical, Cambridge, MA), 5 µM human Ubc4 (E2) produced in bacteria as a hexahistidine fusion as described (Leverson *et al.*, 2000), 10 µM bovine ubiquitin (Sigma-Aldrich), and 2 mM ATP in a 10-µl final volume of 50 mM Tris-HCl, pH 7.5, 2.5 mM $MgCl_2$, and 0.5 mM EDTA for 90 min at room temperature (~23°C). Reactions were stopped with 2× SDS–PAGE sample buffer, resolved on 3–8% Tris-acetate gels (Invitrogen, Carlsbad, CA), and analyzed by immunoblotting with anti-ubiquitin antibody (Sigma-Aldrich) or anti-hemagglutinin (12CA5).

Immunofluorescence techniques and microscopy

GFP or red fluorescent protein (RFP)–fusion proteins were observed in cells after fixation with cold methanol or in live cells. DNA was visualized with 4′,6-diamidino-2-phenylindole (DAPI; Sigma-Aldrich) at 2 µg/ml. Indirect immunofluorescence microscopy was done as described previously (Balasubramanian *et al.*, 1997). Primary antibodies used were TAT-1 monoclonal antibody (1:200; a gift from K. Gull, University of Oxford, Oxford, United Kingdom) for tubulin detection and mouse anti-GFP antibody (1:100; Roche, Indianapolis, IN) for detection of GFP-tagged proteins. Secondary Cy3-conjugated anti-mouse antibody (1:2000; Chemicon, Temecula, CA) and BODIPY FL–conjugated anti-mouse antibody (1:100; Molecular Probes) were used. Photomicrographs were obtained using an Eclipse E600 fluorescence microscope (Nikon, Melville, NY) coupled to a cooled charge-coupled device (CCD) camera (ORCA-ER; Hamamatsu Photonics, Hamamatsu, Japan), and image processing and analysis was carried out using IPLab Spectrum software (Signal Analytics, Vienna, VA).

For quantitative microscopy, GFP, RFP, and mCherry fusion proteins were imaged live on a spinning disk confocal microscope (UltraView LCI; PerkinElmer, Waltham, MA) with a 100×/numerical aperture 1.40 Plan Apochromat oil immersion objective. A 488-nm argon ion laser was used for GFP, and a 594-nm helium neon laser was used for RFP and mCherry fusion proteins. Images were collected using a CCD camera (ORCA-ER) and processed using MetaMorph 7.1 software (MDS Analytical Technologies, Sunnyvale, CA). Average fluorescence intensities were measured using ImageJ software (National Institutes of Health, Bethesda, MD), and final values are expressed as green/red ratios.

ACKNOWLEDGMENTS

We are grateful to Jian-qiu Wu, Takashi Toda, Susan Forsburg, Ian Hagan, Kenneth E. Sawin, Janet L. Paluh, and the Yeast Genetic Resource Center (Osaka, Japan) for providing yeast strains or plasmids and K. Gull for providing TAT1 antibodies. We thank Rui-chuan Chen for his helpful suggestions on biochemical experiments and Sheng-wei Yu, Tong-tong Li, Meng-ting Zhang, and Fu-jun Peng for their help in constructing some yeast strains. A.E.J. was supported by the Cellular, Biochemical, and Molecular Sciences Training Program, National Institutes of Health, Grant T32 GM08554. This work was supported by National Institutes of Health Grant GM058406-11 to D.M.; the Howard Hughes Medical Institute, of which K.L.G. is an investigator; and grants from the National Natural Science Foundation of China (30771078 and 30871376), Key Project of Chinese Ministry of Education (108076), and the Young Outstanding Investigator Program of Fujian Province (2007F3098) to Q.W.J. This work was also supported by grants from the Science Planning Program of Fujian Province (2009J1010) and by the 111 Project of Education of China (B06016).

REFERENCES

Bahler J, Steever AB, Wheatley S, Wang Y, Pringle JR, Gould KL, McCollum D (1998a). Role of polo kinase and Mid1p in determining the site of cell division in fission yeast. J Cell Biol 143, 1603–1616.

Bahler J, Wu JQ, Longtine MS, Shah NG, McKenzie A 3rd, Steever AB, Wach A, Philippsen P, Pringle JR (1998b). Heterologous modules for efficient and versatile PCR-based gene targeting in *Schizosaccharomyces pombe*. Yeast 14, 943–951.

Balasubramanian MK, McCollum D, Gould KL (1997). Cytokinesis in fission yeast *Schizosaccharomyces pombe*. Methods Enzymol 283, 494–506.

Brooks L 3rd, Heimsath EG Jr, Loring GL, Brenner C (2008). FHA-RING ubiquitin ligases in cell division cycle control. Cell Mol Life Sci 65, 3458–3466.

Carnahan RH, Gould KL (2003). The PCH family protein, Cdc15p, recruits two F-actin nucleation pathways to coordinate cytokinetic actin ring formation in *Schizosaccharomyces pombe*. J Cell Biol 162, 851–862.
Castiel A, Danieli MM, David A, Moshkovitz S, Aplan PD, Kirsch IR, Brandeis M, Kramer A, Izraeli S (2011). The Stil protein regulates centrosome integrity and mitosis through suppression of Chfr. J Cell Sci 124, 532–539.
Chang L, Gould KL (2000). Sid4p is required to localize components of the septation initiation pathway to the spindle pole body in fission yeast. Proc Natl Acad Sci USA 97, 5249–5254.
Chin CF, Yeong FM (2010). Safeguarding entry into mitosis: the antephase checkpoint. Mol Cell Biol 30, 22–32.
Fankhauser C, Marks J, Reymond A, Simanis V (1993). The *S. pombe* cdc16 gene is required both for maintenance of p34cdc2 kinase activity and regulation of septum formation: a link between mitosis and cytokinesis?. EMBO J 12, 2697–2704.
Fong CS, Sato M, Toda T (2010). Fission yeast Pcp1 links polo kinase-mediated mitotic entry to gamma-tubulin-dependent spindle formation. EMBO J 29, 120–130.
Fraschini R, Bilotta D, Lucchini G, Piatti S (2004). Functional characterization of Dma1 and Dma2, the budding yeast homologues of *Schizosaccharomyces pombe* Dma1 and human Chfr. Mol Biol Cell 15, 3796–3810.
Gietz RD, Schiestl RH, Willems AR, Woods RA (1995). Studies on the transformation of intact yeast cells by the LiAc/SS-DNA/PEG procedure. Yeast 11, 355–360.
Gould KL, Ren L, Feoktistova AS, Jennings JL, Link AJ (2004). Tandem affinity purification and identification of protein complex components. Methods 33, 239–244.
Guertin DA, Trautmann S, McCollum D (2002a). Cytokinesis in eukaryotes. Microbiol Mol Biol Rev 66, 155–178.
Guertin DA, Venkatram S, Gould KL, McCollum D (2002b). Dma1 prevents mitotic exit and cytokinesis by inhibiting the septation initiation network (SIN). Dev Cell 3, 779–790.
James P, Halladay J, Craig EA (1996). Genomic libraries and a host strain designed for highly efficient two-hybrid selection in yeast. Genetics 144, 1425–1436.
Jin QW, Ray S, Choi SH, McCollum D (2007). The nucleolar Net1/Cfi1-related protein Dnt1 antagonizes the septation initiation network in fission yeast. Mol Biol Cell 18, 2924–2934.
Johnson AE, Gould KL (2011). Dma1 ubiquitinates the SIN scaffold, Sid4, to impede the mitotic localization of Plo1 kinase. EMBO J 30, 341–354.
Kang D, Chen J, Wong J, Fang G (2002). The checkpoint protein Chfr is a ligase that ubiquitinates Plk1 and inhibits Cdc2 at the G2 to M transition. J Cell Biol. 156, 249–259.
Keeney JB, Boeke JD (1994). Efficient targeted integration at leu1-32 and ura4-294 in *Schizosaccharomyces pombe*. Genetics 136, 849–856.
Krapp A, Gulli MP, Simanis V (2004). SIN and the art of splitting the fission yeast cell. Curr Biol 14, R722–R730.
Leverson JD, Joazeiro CA, Page AM, Huang H, Hieter P, Hunter T (2000). The APC11 RING-H2 finger mediates E2-dependent ubiquitination. Mol Biol Cell 11, 2315–2325.
Loring GL, Christensen KC, Gerber SA, Brenner C (2008). Yeast Chfr homologs retard cell cycle at G1 and G2/M via Ubc4 and Ubc13/Mms2-dependent ubiquitination. Cell Cycle 7, 96–105.
MacCoss MJ *et al.* (2002). Shotgun identification of protein modifications from protein complexes and lens tissue. Proc Natl Acad Sci USA 99, 7900–7905.
Maundrell K (1993). Thiamine-repressible expression vectors pREP and pRIP for fission yeast. Gene 123, 127–130.
McCollum D, Gould KL (2001). Timing is everything: regulation of mitotic exit and cytokinesis by the MEN and SIN. Trends Cell Biol 11, 89–95.
Moreno S, Klar A, Nurse P (1991). Molecular genetic analysis of fission yeast *Schizosaccharomyces pombe*. Methods Enzymol 194, 795–823.
Morrell JL *et al.* (2004). Sid4p-Cdc11p assembles the septation initiation network and its regulators at the *S. pombe* SPB. Curr Biol 14, 579–584.
Mulvihill DP, Petersen J, Ohkura H, Glover DM, Hagan IM (1999). Plo1 kinase recruitment to the spindle pole body and its role in cell division in *Schizosaccharomyces pombe*. Mol Biol Cell 10, 2771–2785.
Murone M, Simanis V (1996). The fission yeast dma1 gene is a component of the spindle assembly checkpoint, required to prevent septum formation and premature exit from mitosis if spindle function is compromised. EMBO J 15, 6605–6616.
Ohkura H, Hagan IM, Glover DM (1995). The conserved *Schizosaccharomyces pombe* kinase plo1, required to form a bipolar spindle, the actin ring, and septum, can drive septum formation in G1 and G2 cells. Genes Dev 9, 1059–1073.
Pryciak PM, Hartwell LH (1996). AKR1 encodes a candidate effector of the G beta gamma complex in the *Saccharomyces cerevisiae* pheromone response pathway and contributes to control of both cell shape and signal transduction. Mol Cell Biol 16, 2614–2626.
Rigaut G, Shevchenko A, Rutz B, Wilm M, Mann M, Seraphin B (1999). A generic protein purification method for protein complex characterization and proteome exploration. Nat Biotechnol 17, 1030–1032.
Scolnick DM, Halazonetis TD (2000). Chfr defines a mitotic stress checkpoint that delays entry into metaphase. Nature 406, 430–435.
Summers MK, Bothos J, Halazonetis TD (2005). The CHFR mitotic checkpoint protein delays cell cycle progression by excluding Cyclin B1 from the nucleus. Oncogene 24, 2589–2598.
Tanaka K, Petersen J, MacIver F, Mulvihill DP, Glover DM, Hagan IM (2001). The role of Plo1 kinase in mitotic commitment and septation in *Schizosaccharomyces pombe*. EMBO J 20, 1259–1270.
Tasto JJ, Carnahan RH, McDonald WH, Gould KL (2001). Vectors and gene targeting modules for tandem affinity purification in *Schizosaccharomyces pombe*. Yeast 18, 657–662.
Trautmann S, Wolfe BA, Jorgensen P, Tyers M, Gould KL, McCollum D (2001). Fission yeast Clp1p phosphatase regulates G2/M transition and coordination of cytokinesis with cell cycle progression. Curr Biol 11, 931–940.
Tuttle RL, Bothos J, Summers MK, Luca FC, Halazonetis TD (2007). Defective in mitotic arrest 1/ring finger 8 is a checkpoint protein that antagonizes the human mitotic exit network. Mol Cancer Res 5, 1304–1311.
Yu X *et al.* (2005). Chfr is required for tumor suppression and Aurora A regulation. Nat Genet 37, 401–406.